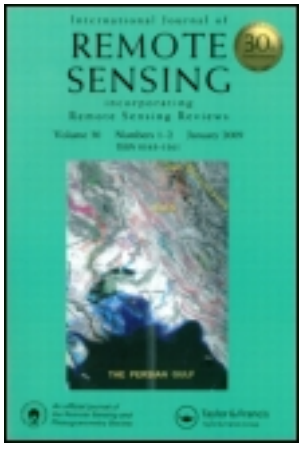

International Journal of Remote Sensing

Publication details, including instructions for authors and subscription information:
http://www.tandfonline.com/loi/tres20

Aboveground biomass estimation in intervened and non-intervened Nothofagus pumilio forests using remotely sensed data

Marcela Poulain [a], Marco Peña [b], Andreas Schmidt [a], Harald Schmidt [c] & Andreas Schulte [a]

[a] Wald-Zentrum, Institute of Landscape Ecology, Westfälische Wilhelms- Universität Münster, 48149, Münster, Germany

[b] Centro de Estudio de Recursos Naturales Oterra, Universidad Mayor, Santiago, Chile

[c] Faculty of Forest Science, Universidad de Chile, Santiago, Chile

Available online: 08 Dec 2011

To cite this article: Marcela Poulain, Marco Peña, Andreas Schmidt, Harald Schmidt & Andreas Schulte (2012): Aboveground biomass estimation in intervened and non-intervened Nothofagus pumilio forests using remotely sensed data, International Journal of Remote Sensing, 33:12, 3816-3833

To link to this article: http://dx.doi.org/10.1080/01431161.2011.635716

International Journal of Remote Sensing
Vol. 33, No. 12, 20 June 2012, 3816–3833

Taylor & Francis
Taylor & Francis Group

Aboveground biomass estimation in intervened and non-intervened *Nothofagus pumilio* forests using remotely sensed data

MARCELA POULAIN*†, MARCO PEÑA‡, ANDREAS SCHMIDT†, HARALD SCHMIDT§ and ANDREAS SCHULTE†

†Wald-Zentrum, Institute of Landscape Ecology, Westfälische Wilhelms- Universität Münster, 48149 Münster, Germany

‡Centro de Estudio de Recursos Naturales Oterra, Universidad Mayor, Santiago, Chile

§Faculty of Forest Science, Universidad de Chile, Santiago, Chile

(*Received 31 December 2009; in final form 24 October 2011*)

Forest inventory data can be used along with remotely sensed data to estimate biomass and carbon stocks over large and inaccessible forested areas. In this study, the relationship between satellite-derived multispectral data and forest variables from intervened and non-intervened *Nothofagus pumilio* forest stands located in the Magellan region of Chile was examined, in order to quantify the over bark volume (OBV) and aboveground tree biomass (AGTB). Four vegetation parameters – the green normalised difference vegetation index (GNDVI), normalised difference vegetation index (NDVI), simple ratio (SR) and vegetation cover fraction (VCF) – were retrieved from an Advanced Spaceborne Thermal Emission and Reflection Radiometer (ASTER) image of the study area. The results indicate that only the VCF presents significant differences among intervened and non-intervened stands. The best OBV and AGTB models ($R^2 = 0.58$) were found using the SR index and the VCF as predictors. This result could be transferred to estimate biomass and volume in other *Nothofagus pumilio* forests with similar conditions. Moreover, it can be used to assess temporal carbon changes.

1. Introduction

Forests play an important role in global carbon cycling, as they are large pools of carbon as well as potential carbon sinks and sources to the atmosphere (Schulte 2001, Muukkonen and Heiskanen 2007). Furthermore, biomass can provide information about the condition of the forest stands and thus can be used not only in carbon cycle studies, but also to support management operations such as land-use policy, prediction of forest fire behaviour or assessment of insect infestations (Aronoff 2005).

The reports of carbon stocks and stock temporal changes during the Kyoto Protocol's first commitment period (2008–2012) and the emerging field of carbon trading have put additional demands on methods for estimating carbon sources and sinks (Krankina *et al*. 2004, Poulain *et al*. 2008). Forest inventories and remote sensing are two data sources that can be used to estimate biomass and carbon stocks in forests. Currently, aboveground forest biomass is estimated using inventory data from field sample plots (Brown 2001). Nevertheless, this method is destructive, labour-intensive,

*Corresponding author. Email: marcela.poulain@wald-zentrum.de

International Journal of Remote Sensing
ISSN 0143-1161 print/ISSN 1366-5901 online © 2012 Taylor & Francis
http://www.tandf.co.uk/journals
http://dx.doi.org/10.1080/01431161.2011.635716

time-consuming and expensive (Brown 2002, Zianis and Mencuccini 2003), so a suitable method is required to update forest inventory with the current forest conditions (Wulder *et al*. 2004). Optical multispectral imagery may provide some of the required information for updating forest inventories by reducing the above-mentioned disadvantages. However, in managed forests, the relationship between spectral reflectance and important stand characteristics throughout different site conditions is still not well documented (Lu *et al*. 2004). Consequently, the validity of remotely sensed data must be empirically proven for different species at different geographic locations and under different management strategies.

Most of the biomass and carbon storage studies have been conducted in the northern hemisphere forest ecosystems. Comparable above- and below-ground data for southern hemisphere old-growth forests, such as those dominated by the genus *Nothofagus* (occurring in Argentina, Australia, Chile, New Guinea and New Zealand), are much more limited (Veblen *et al*. 1996, Hart *et al*. 2003). *Nothofagus pumilio* (Poepp. et Endl.) Krasser (lenga) is a medium shade-intolerant deciduous tree species growing in pure or mixed stands in Argentina and Chile. In Chile's Magellan region, lenga forests cover an area of more than 1 100 000 ha, representing 43% of the total land cover in this region (CONAF-CONAMA 1999). These forests represent the most important resources for the regional wood industry (Rosenfeld *et al*. 2006, Klein *et al*. 2008a), and as such these forests were initially intervened, applying the exploitative cut. This harvest practice is based on the selective cut of the better timber trees of the stand, which degrades forest quality and impoverishes future potential timber productivity of the stand (Martínez-Pastur *et al*. 2000). Since 1992, Chilean forestry law allows the use of only shelterwood and selective cutting in lenga forests. Accordingly, the National Forestry Corporation of Chile (CONAF) suggests the use of shelterwood cutting in the lenga forest of the Magellan's region in its technical regulations for silviculture management (Rosenfeld *et al*. 2006). This practice transforms virgin forest into a regular managed one, resulting in higher size increments, better stand health and wood quality, and improved harvesting index (Schmidt and Urzúa 1982).

There is a need for more research on biomass and carbon stocks in large areas in order to understand the management effects on forests, especially the effects of conversion from primary to managed forest. The biomass and carbon storage in *Nothofagus* forests have been studied in New Zealand forests (e.g. Davis *et al*. 2003, Hart *et al*. 2003) and in specific lenga forests (e.g. Caldentey 1995, Loguercio 2001, Weber 2001, Klein *et al*. 2008a,b, Schmidt *et al*. 2008). However, only a few studies have attempted to investigate biomass and carbon storage using optical multispectral imagery in these temperate forests. Moreover, few studies have analysed the differences between such imagery and both intervened and non-intervened stands. Typically, optical multispectral imagery provides spectral wavelengths sensitive to the amount and quality of vegetation canopy foliage, thus providing a tool to assess forest biomass and carbon stocks. Because of their intrinsic spectral resolution and sensitivity, this type of remotely sensed data (e.g. indices) allows the analysis and assessment of the vegetation condition and cover, based on the same spectral sampling intervals or bands. Hence, a strong correlation should be expected between them. Nonetheless, there is vast research demonstrating that in spite of their spectral similarities, these measures may render different results according to the particularities of the study case (e.g. vegetation cover and health status, species composition, physiognomic type, phenologic type) (Treitz and Howarth 1999, Gitelson *et al*. 2002, Le Maire *et al*. 2004). Therefore,

it is important to investigate the relationship between these indices and the *Nothofagus pumilio* forest as a first step in the remotely sensed analysis.

The main objectives of this study are (1) to estimate volume and biomass in a large *Nothofagus pumilio* forest area located in the Magellan region, Chile, by using an equation model integrating forest inventory, remotely sensed data acquired by the Advanced Spaceborne Thermal Emission and Reflection Radiometer (ASTER) and the national forest land-cover map, and (2) to analyse the relationships between some well-known vegetation parameters derived from optical multispectral imagery and the different forest stands (i.e. primary, exploitative and shelterwood cuts stands), estimated by the equation model.

2. Materials and methods

2.1 *Study area*

This study was carried out between summer 2006–2007 and summer 2007–2008 on the oriental slope of the Andes mountain in the Province of Última Esperanza, XII Magallanes y Antártica Chilena region, Chile, at coordinates range between 52° 05′ S – 52° 10′ S, and 71° 35′ W – 71° 55′ W (see figure 1). The study area is a continuum of pure lenga forests of about 20 150 ha. The forests are primary as well as intervened forests, managed by shelterwood cutting by forestry companies.

The mean annual temperature is 5°C, and an average annual precipitation of 596 mm is homogenously distributed throughout the year (Schmidt *et al*. 2003). The topography of the area corresponds to gently undulating hillocks with elevation

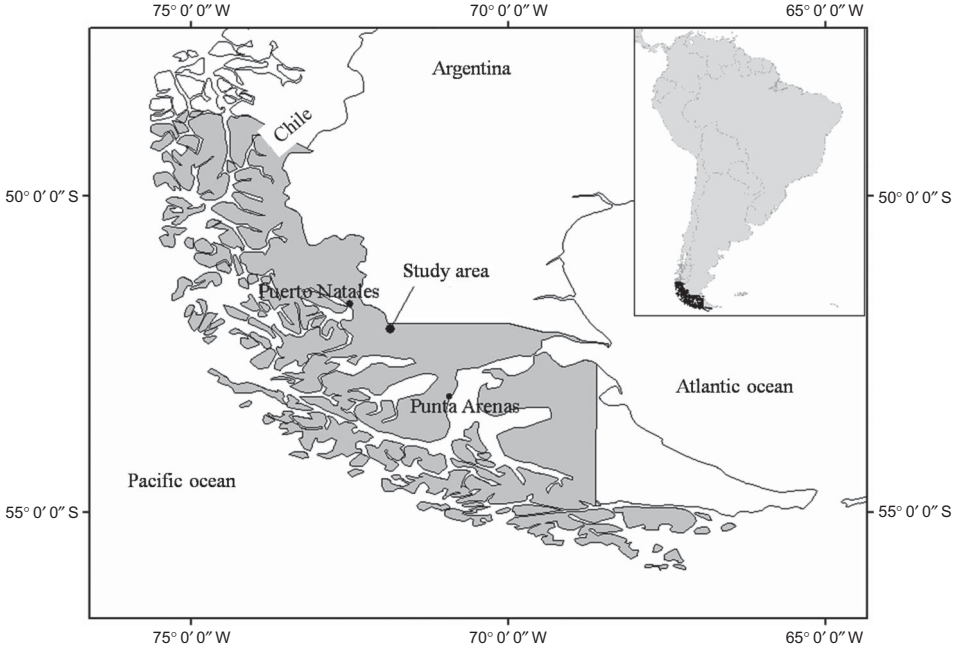

Figure 1. Location of the study area. *Nothofagus pumilio* forest in the Magellan region of Chile.

ranging from 350 to 480 m.a.s.l. (Schmidt *et al*. 2003). Natural vegetation in this sector corresponds to the deciduous forest of Magallanes vegetal formation in the Andean patagonia forest region, patagonia mountain range subregion (Gajardo 1994).

2.2 *Field data collection*

The field data were collected from randomly sampled 500 m^2 circular plots ($n = 166$). The Global Positioning System (GPS) was used to determine the spatial location of each plot centre (GPS measurements were averaged over several minutes to enhance accuracy). Diameter at breast height (DBH) was measured on all stems ≥ 10 cm, along with the tree density and height of dominant trees (DH), used to calculate basal area (BA), over bark volume (OBV) (wood volume including bark), stem biomass (SB) and aboveground tree biomass (AGTB), using the models provided by Loguercio (2001). In addition, the sample plots were classified according to four forest management stages (i.e. silvicultural activity type and year of activity), representing different subsets of forest conditions: non-intervened primary forest stands (P), stands subjected recently to shelterwood cutting (after 2000) (SC1), stands after shelterwood cutting carried out between 1992 and 2000 (SC2) and stands after exploitative cuts applied before 1992 (E). The general characteristics of these forest stands are given in table 1.

2.3 *Remotely sensed data*

An ASTER image acquired on 5 October 2006 was used. This image is composed of two visible bands, one near infrared band (VNIR), six short-wave infrared bands (SWIR) and five thermal infrared bands (TIR). The scene dimension is 60 km $\times$ 60 km, and the spatial resolution is 15 m for VNIR bands, 30 m for SWIR bands and 90 m for TIR bands. For the purposes of this work, all the reflected bands (i.e. VNIR and SWIR) were useful. The selected ASTER image was considered optimum for the purposes of this work, because it was acquired during a cloudless period in which the *Nothofagus pumilio* forest reaches its most vigorous condition (i.e. spring), which is also compatible with the time that field data were collected. Further, the image

Table 1. Details of the sample plots in the study area ($n = 166$).

	P		SC1		SC2		E	
Forest variable	Mean	SE	Mean	SE	Mean	SE	Mean	SE
Dominant height (m)	20	0.4	21	0.4	21	0.7	21	0.5
Density (trees ha^{-1})	560	40.9	263	30.7	213	27.0	437	41.3
Basal area (m^2 ha^{-1})	55.2	2.2	38.9	2.3	33.4	2.8	46.4	3.2
Over bark volume (m^3 ha^{-1})	498.1	21.7	374.5	20.1	321.5	30.2	444.5	33.4
Stem biomass (Mg ha^{-1})	215.0	8.6	159.8	10.2	138.7	12.4	183.7	12.9
Aboveground tree biomass (Mg ha^{-1})	267.1	10.6	199.8	13.0	174.0	15.7	228.8	16.2

Note: P is a non-intervened forest stand ($n = 66$), SC1 is a stand subjected recently to the shelterwood cut method (after 2000) ($n = 33$), SC2 is a stand after the shelterwood cut method carried out between 1992 and 2000 ($n = 28$), E is a stand after exploitative cuts applied before 1992 ($n = 39$). SE is the standard error.

to be used should be chosen with consideration to the date of inventory data acquisition, as the study area is continually subjected to forest management. The continual harvest of the lenga stands presents changes that, if not synchronized with the time of field data collection and the land-cover map, could significantly compromise accurate representation. Only the image matching these conditions could be selected.

2.4 *Image processing*

To minimize and eliminate the main image's geometric distortions, a non-parametric correction based on a triangulation model with a nearest neighbour resampling (at the spatial resolution of VNIR bands) was performed. This was automatically made with the ENVI 4.3 software by reading the geometric model and satellite orbit parameters contained in the image's metadata. The geographic coordinates of the output image were Universal Tranverse Mercator (UTM) and World Geodetic Datum 1984 (WGS84).

To minimize and eliminate the extraneous path radiance added to the image as a result of the haze effect (caused by atmospheric scattering) and adjacency effect (caused by reflection from nearby surfaces), the Fast Line-of-sight Atmospheric Analysis of Spectral Hypercubes (FLAASH) model was used. This model calculates the atmospheric transmittance of radiation based on the Moderate Resolution Atmospheric Transmission (MODTRAN) algorithm. The units of the output image were proportional to the apparent surface reflectances.

To compensate the image's illumination differences affecting the reliability of the vegetation cover fraction (VCF) values, reflectance bands were subjected to a topographic normalization by using a lambertian reflectance model available in ERDAS 9.1 software. This model requires the solar geometry at the image acquisition time (i.e. azimuth and elevation angles), as well as a digital elevation model (DEM), which allows the creation of a hill-shading image of the terrain relief depicted in the image. To generate the DEM, ASTER 3n (nadir viewing) and 3b (off-nadir viewing) bands were used as left and right rational polynomial coefficient-positioned stereo imagery, respectively. Forty-five tie points with a y-parallax error inferior to one pixel were used to calculate the epipolar geometry and images for extracting the DEM, which was automatically georeferenced to the UTM, WGS84 coordinates system and resampled at the spatial resolution of VNIR bands. Incorrect DEM elevation values were eliminated by applying a noise removal procedure, in which values greater than two standard deviations of the mean of a 3×3 pixel window size were replaced with the median computed for those surrounding pixels.

Three greenness vegetation indices and the VCF (from now vegetation parameters) were retrieved from the ASTER image. The vegetation indices used in this study are described in table 2.

VCF was derived from the illumination-normalised reflectances by applying a linear spectral unmixing technique, which determines the proportion of each pixel occupied by vegetation. This approach assumes that the pixel reflectance value of the image is a linear combination of the reflectance of each predominant material (i.e. endmember) present within a pixel.

As the study area is composed of quite distinctive materials, an unsupervised classification allowed a clear delineation of the representative training sites of vegetation, bare soil, ice/snow and water. These end members were entered into the unmixing algorithm.

Table 2. Vegetation indices used in this study.

Vegetation index	Equation	Reference
Normalised difference vegetation index (NDVI)	(NIR – RED)/(NIR + RED)	Rouse *et al*. (1973)
Green difference vegetation index (GNDVI)	(NIR – GREEN)/(NIR + GREEN)	Gitelson *et al*. (1996)
Simple ratio (SR)	NIR/RED	Birth and McVey (1968)

Note: GREEN is the visible green band (ASTER band 1, spectral range 0.52–0.60 μm), RED is the visible red band (ASTER band 2, spectral range 0.63–0.69 μm) and NIR is the near infrared band (ASTER band 3, spectral range 0.76–0.86 μm).

For a given spectral band, the reflectance of a given pixel is expressed by the following equation (Lillesand *et al*. 2004):

$$r_\lambda = f_1 r_{1\lambda} + \ldots + f_n r_{n\lambda} + e_\lambda, \quad (1)$$

where r_λ is the composite reflectance observed in band λ; $f_1, \ldots, f_n$ are fractions of the pixel occupied by each of the n end members; $r_{1\lambda}, \ldots, r_{n\lambda}$ are reflectances that would be observed if a pixel were completely covered by the corresponding end member, and e_λ is the error term for band λ.

The Jeffries-Matusita and divergence transformed measures were applied to test the statistical separability between the spectral patterns of all pairs of end members. The root mean square error (RMSE) image yielded for the unmixed algorithm was inspected to refine poorly represented endmembers (i.e. areas with high RMSE) by redelineating their corresponding training sites.

2.5 *Statistical analysis*

The assumptions for normality and homogeneity of variance were examined by using the Kolmogorov-Smirnov non-parametric test and the Levené test, respectively. A one-way analysis of variance (ANOVA) and the respective post-hoc tests were used to test for significant differences in forest variables and vegetation parameters across the forest stands ($p < 0.05$). The Tukey post-hoc test was used for homogeneous variances, and Tamhane's T2 test was used for nonhomogeneous variances.

In the same study area, Poulain *et al*. (2010) tested eight regression models (linear and non-linear) for estimating lenga forest variables. The best two models rendered in that research were selected for this study (see table 3) and examined with a field data subset (138 sample plots) of the study area in order to estimate the BA, OBV, SB and AGTB (DBH $\geq$ 10 cm). Vegetation parameters were incorporated as independent variables, and forest stand variables from 138 sample plots were incorporated as dependent variables. These regression models were tested taking into account all possible combinations of independent variables (the normalised difference vegetation index (NDVI), green normalised difference vegetation index (GNDVI), simple ratio (SR) and VCF) for each dependent variable considered. Outliers were identified and removed from the data set using scatter plot analysis and studentized residual threshold values >3.0. Values are given with the corresponding standard error (SE). Statistical analyses were carried out using SPSS 15.0.

Table 3. Regression models tested in this study.

Model	Equation	References
M1	$y = a + bx + cx^2$	Labrecque *et al*. (2006)
M2	$y = (1 + x_1)^a\, x_2{}^b \exp(c + dx_1 + ex_2)$	Muukkonen and Heiskanen (2005)

Note: a, b, c, d and e are parameters, x, x_1 and x_2 are the independent variables (remote-sensing data: NDVI, GNDVI, SR and VCF) and y is the dependent variable (forest variable: basal area (BA), over bark volume (OBV), stem biomass (SB) and aboveground tree biomass (AGTB)).

Estimation performance for BA, OBV, SB and AGTB were evaluated by calculating the coefficient of determination (R^2), showing the proportion of the total variability in the dependent variable explained by the model:

$$R^2 = \frac{1 - S_\mathrm{r}}{S_\mathrm{c}}, \tag{2}$$

where S_r is the residual sum of squares and S_c the corrected sum of squares.

Besides the 138 sample plots applied to develop the biomass equation models, a subsample of 28 plots of the field data set was used for independent validation, using the statistics RMSE, which states the accuracy of the estimates for the forest variables:

$$\mathrm{RMSE} = \sqrt{\frac{1}{n}\sum_{i=1}^{n}(\hat{y}_i - y_i)^2}, \tag{3}$$

where $\hat{y}$ is an estimated variable, y is the field (measured) variable and n is the number of observations.

The validation was also carried out using the mean percentage standard error (S), which indicates the size of error as a percentage of the mean of the estimated variable distribution:

$$S\% = \frac{100}{n}\sum\frac{|y - \hat{y}|}{\hat{y}}, \tag{4}$$

where y represents observed values and $\hat{y}$ represents predicted values.

In sum, the comparison of the different fitted models was based on the R^2, RMSE and S values. The equation models were tested using all the sample plots in the study area and in each of the four classes of forest management (P, SC1, SC2 and E).

Land-cover maps of lenga corresponding to the four classes of forest management stands were extracted from the national forest land-cover map (CONAF-CONAMA 2006) and the land-cover map of the study area of the Forestal y Ganadera Monte Alto Ltda company. This classified thematic layer was overlaid to each vegetation parameter, in order to apply the regression models and to estimate BA, OBV, SB and AGTB for each class of lenga forest in all the study area (20 149 km^2). Pixels corresponding to non-forested lands that were included by the thematic layer boundaries (edge pixels, mostly) were excluded from the analysis.

3. Results

3.1 *Forest stands data*

Based on field data, the dominant height of the trees in the study area varied from 14 to 32 m, tree density from 14 to 1 747 trees ha^{-1}, BA from 2.6 to 86.9 m^2 ha^{-1}, OBV from 25.2 to 947.7 m^3 ha^{-1}, SB from 10 to 344 Mg ha^{-1} and AGTB from 13 to 429 Mg ha^{-1}. The SE in all the forest variables is high because the study area consists of primary and managed stands in different growing phases. Stands after an exploitative cut (E) showed the highest SE in BA (3.2), OBV (33.4), SB (12.9) and AGTB (16.2), as compared to the other stands (see table 1). This can be explained by the exploitative interventions, which irregularly transform the forest into one containing fragmented patches of isolated regeneration (Martínez-Pastur *et al*. 2000). There were no significant differences in BA, OBV, BS and AGTB between the primary and the exploitative stands (see table 4). Furthermore, there was also no significant difference in all the forest variables across the two shelterwood cut stands types SC1 and SC2 and between SC1 and E stands.

3.2 *Forest stands and vegetation parameters*

No significant differences were found in the NDVI and GNDVI values between the stands P, SC1 and E, whereas significant differences showed for both index values between the two shelterwood cut stands (see table 5). VCF values observed in stand SC2 were significantly different from those in stands P, SC1 and E, whereas the same parameter presented no significant differences between primary and exploitative stands, and also between stand SC1 with E. Moreover, there were no significant differences in the SR across the four stands ($F = 2.33$).

3.3 *Regression models and stands variables estimation*

The best R^2 values from the different equations were 0.67 for BA, 0.59 for OBV, 0.68 for SB, and 0.68 for AGTB. For the four forest variables, SR showed the best performance in the regression equations with one predictive variable, and the combination between SR and VCF achieved the best behaviour in the equation with two independent variables (see table 6). NDVI and GNDVI performed poorly in the two equation models.

Table 4. Significant differences of the forest variables in the forest stands.

Stand	BA	OBV	SB	AGTB
P	*a*	*a*	*a*	*a*
SC1	*bc*	*bc*	*bc*	*bc*
SC2	*c*	*c*	*c*	*c*
E	*ba*	*ab*	*ba*	*ba*
F	15.19	9.1	10.98	10.39

Note: Different letters indicate significant differences ($p \leq 0.05$) between forest stands for the same vegetation parameters. P is a non-intervened forest stand, SC1 is a stand subjected recently to the shelterwood cut method (after 2000), SC2 is a stand after the shelterwood cut method carried out between 1992 and 2000, E is a stand after exploitative cuts applied before 1992. *F* is the Fisher test.

Table 5. Significant differences of the vegetation parameters in the forest stands.

Stand	NDVI	GNDVI	SR	VCF
P	*ab*	*ab*	*a*	*a*
SC1	*a*	*a*	*a*	*b*
SC2	*b*	*b*	*a*	*c*
E	*ab*	*ab*	*a*	*ab*
F	2.71	3.94	2.33	13.8

Note: Different letters indicate significant differences ($p \leq 0.05$) between forest stands for the same vegetation parameters. P is a non-intervened forest stand, SC1 is a stand subjected recently to the shelterwood cut method (after 2000), SC2 is a stand after the shelterwood cut method carried out between 1992–2000, E is a stand after exploitative cuts applied before 1992. *F* is the Fisher test.

Table 6. The best regression models of the basal area (BA), over bark volume (OBV), stem biomass (SB) and aboveground tree biomass (AGTB) in a *Nothofagus pumilio* forest ($n = 166$).

Dependent variable	Model	Predictive	Parameters					R^2
			a	*b*	*c*	*d*	*e*	
BA	M1	SR	−300.195	180.972	−22.455			0.67
OBV	M1	SR	−2337.292	1381.126	−158.53			0.59
OBV	M2	SR/VCF	0.866	−0.0000000064	5.167	−0.076	−0.078	0.58
SB	M1	SR	−1071.331	627.091	−72.013			0.68
SB	M2	SR/VCF	−23.966	−0.00000055	17.425	7.14	−0.727	0.42
AGTB	M1	SR	−1317.201	766.223	−86.671			0.68
AGTB	M2	SR/VCF	−4.759	−0.00000012	7.673	1.505	−0.234	0.58

Note: M1 is the model $y = a + bx + cx^2$ and M2 is the model $y = (1 + x_1)^a\ x_2{}^b \exp(c + dx_1 + ex_2)$.

The AGTB is plotted against the SR values in figure 2. The relationship between both is relatively linear. Regarding the basal area estimation, for all the stands, model 1 (Labrecque *et al*. 2006) provided the best results ($R^2 = 0.67$ and for the validation subsample RMSE = ±25.8 $m^2\ ha^{-1}$ and $S = 128.3$), although the *S* value indicated that this model is not an adequate estimator for this forest variable, whereas only for stand SC1, this model showed a high RMSE (±12.9 $m^2\ ha^{-1}$) and a low *S* (29.1). It is assumed that only for this stand (SC1), could the basal area be estimated (see table 7).

For all stands, model 2 (Muukkonen and Heiskanen 2005), using SR and VCF as the predictors, provided the best results for the estimation of the over bark volume ($R^2 = 0.58$ and for the validation subsample RMSE = ±178.6 $m^3\ ha^{-1}$ and $S = 35.9$). This model had the best behaviour in stand SC1, when compared with the other stands, in which case, RMSE was ±127.4 $m^3\ ha^{-1}$ and *S* was 23.4.

Model 2 also showed the best results for the stem biomass and aboveground tree biomass estimation ($R^2 = 0.42, 0.58$ and for the validation subsample RMSE = ±91.3, 92.7 Mg ha^{-1}, $S = 47.5, 35.9$, respectively) using SR and VCF as predictors.

The estimation of the OBV, SB and AGTB variables showed that the combination of two vegetation parameters showed better behaviour when compared with a single independent variable. In all the cases, SR and VCF were the best predictors. Models of stands with shelterwood cuts (SC1 and SC2) showed the best behaviours (RMSE and *S*) when compared with non-intervened and exploitative stands (see table 7).

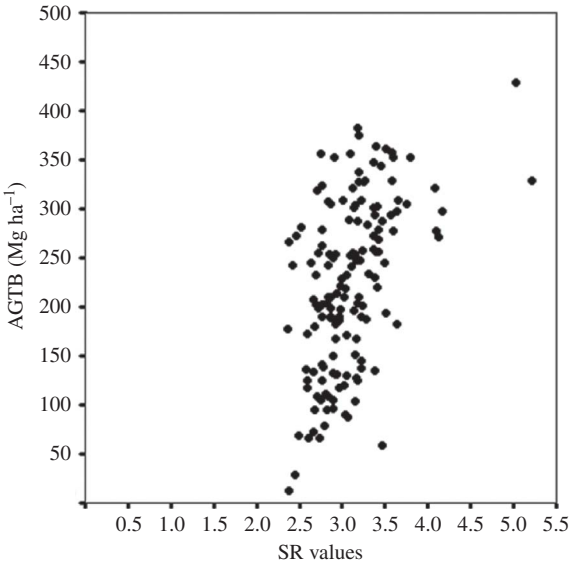

Figure 2. Scatter plot of the aboveground tree biomass (AGTB) and the simple ratio (SR) values.

Applying model 2 (Muukkonen and Heiskanen 2005) for the four forest management stands provides a mean estimation of aboveground tree biomass of 147 Mg ha^{-1} ($\pm$83.7 Mg ha^{-1}) in P stand, 140 Mg ha^{-1} ($\pm$81.4 Mg ha^{-1}) in SC1 stand, 144 Mg ha^{-1} ($\pm$64.6 Mg ha^{-1}) in stand SC2 and 141 Mg ha^{-1} ($\pm$92.4 Mg ha^{-1}) in stand E. For all the study area, the total aboveground tree biomass was approximately 2 930 000 Mg in 20 149 ha. The spatial distribution of the aboveground biomass for the entire surface is shown in figure 3.

4. Discussion

4.1 *Forest stands data*

In this study, the primary forest accounted for the highest aboveground biomass with 267.1 Mg ha^{-1}. Compared with the primary forest, in both stands with shelterwood cuts, the AGTB decreased according to the seed cuts to which both stands were subjected. The seed cut is the first step from the shelterwood cuts system, whose aim is to open the stand sufficiently to promote the establishment and development of natural regeneration. A better microclimatic condition, due to the shelterwood cuts, allows for a better natural regeneration (Caldentey *et al*. 2009). Specifically, after a seed cut, the overall incident sunlight available for regeneration increases four times in comparison with the primary forest (Caldentey *et al*. 2000). Thus, the biomass of regeneration increases with this forest practice. According to Schmidt *et al*. (2009), the total biomass of natural regeneration varied from 0.9 Mg ha^{-1} (0.5 Mg ha^{-1} above and 0.4 Mg ha^{-1} belowground) for the primary forest to 19.5 Mg ha^{-1} (13.6 Mg ha^{-1} above and 5.9 Mg ha^{-1} belowground) 14 years after the seed cut. During the same period, vegetation carbon storage varied, from 0.5 to 9.8 Mg ha^{-1}. These natural regeneration values could increase the assessment of the aboveground tree biomass estimated in this study.

Table 7. Regression models that better performed: RMSE and S of the basal area (BA), stem biomass (SB), over bark volume (OBV) and aboveground tree biomass (AGTB) in different *Nothofagus pumilio* stands ($n = 166$).

			Stand									
			P		SC1		SC2		E		VAL	
Model	Dep. var. (y)	Indep. var (x)	RMSE	S	RMSE	S	RMSE	S	RMSE	S	RMSE	S
M1	BA	SR	22.1	175.2	12.9	29.1	26.9	299.9	24.7	892.2	25.8	128.3
M1	OBV	SR	222.8	79.9	140.7	47.0	285.2	157.1	219.7	55.4	250.2	102.4
M2	OBV	SR/VCF	172.5	34.7	127.4	23.4	129.5	26.6	183.9	35.6	178.6	35.9
M1	SB	SR	96.5	99.4	64.1	81.4	123.9	312.4	86.9	52.8	103.5	129.5
M2	SB	SR/VCF	128.7	40.0	214.5	31.8	58.6	32.2	85.2	47.2	91.3	47.5
M1	AGTB	SR	120.1	102.5	81.3	89.0	158.3	360.8	108.0	52.5	129.7	134.9
M2	AGTB	SR/VCF	83.7	30.1	81.4	27.9	64.6	26.1	92.4	35.1	92.7	35.9

Note: M1 is the tested model: $y = a + bx + cx^2$, M2 corresponds to the tested model: $y = (1 + x_1)^a\ {x_2}^b \exp(c + dx_1 + ex_2)$, Dep. var. is the dependent variable, Indep. var. is the independent variable, P is a non-intervened forest stand, SC1 is a stand subjected recently to shelterwood cut method (after 2000), SC2 is a stand after a shelterwood cut method carried out between 1992–2000, E is a stand after exploitative cuts applied before 1992. VAL is the validation plots set ($n = 28$). RMSE is the root mean square error, and S is the mean percentage standard error.

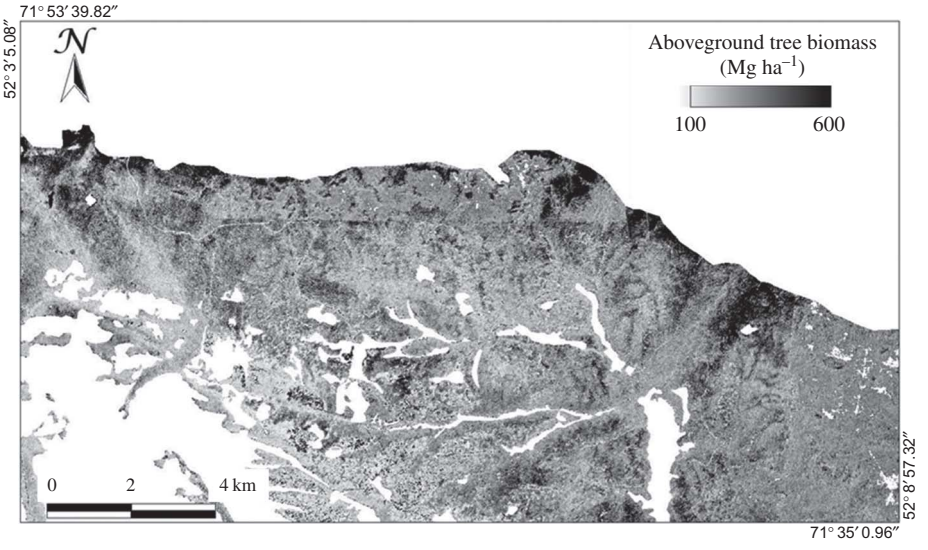

Figure 3. Spatial distribution of *Nothofagus pumilio* aboveground tree biomass utilizing the regression model 2.

The AGTB in the primary forest in this study area was lower than the biomass estimated by Weber (2001) and Loguercio (2001) in Tierra del Fuego Island (382.8 Mg ha^{-1}), Argentina. On the Chilean side of this island, Caldentey (1995) reported aboveground biomass values of 477 Mg ha^{-1}. Slightly lower values, 310.3 to 446.0 Mg ha^{-1}, were reported for *Nothofagus* forests in New Zealand (Veblen *et al*. 1996, Hart *et al*. 2003). One reason for the low AGTB values reported in this work (261.6 Mg ha^{-1}) is that the forest in the study area was managed under exploitative and then under shelterwood cuts. This means that the best forest stands were first harvested, and in the present only the lowest stands are not intervened.

4.2 *Relationship between forest variables and vegetation parameters*

A direct relation (concordance) between the significant differences at the stands in the forest variables and the vegetation parameters was not found (see tables 4 and 5). For example, significant differences in the values of the four forest variables were presented between P and the stands with shelterwood cuts (SC1 and SC2), whereas SR showed no significant differences between all stands. Furthermore, only VCF presented significant differences between all stands; specifically this parameter showed difference between the SC1 and the SC2 stands, whereas the difference between the forest variables was indeterminate.

One reason for these results could be the influence of the understory vegetation cover, in that the vegetation parameters are sensitive to both the reflectance signal of the overstory canopy cover as well as the understory cover, whereas the forest variables only include the overstory canopy cover. This situation can generate errors in the interpretation of the optical remote-sensing data, mainly in the managed stands, because the regeneration cover after a shelterwood cut could be similar to the tree canopy cover. Nevertheless, in lenga stands, Eckert (2006) showed that the influence of the understory on the LAI-reflectance relationship seems to be less than expected.

Furthermore, in the same study area, Poulain *et al*. (2010) found that the influence of background and understory vegetation does not considerably affect the reflectance. Moreover, Wulder *et al*. (2004) pointed out that the residual forest has a different reflectance pattern than the regenerating forest inside the harvested lodgepole pine stands.

4.3 *Regression models and forest variables estimation*

It is necessary to test many combinations of predictor image variables because different forest types require diverse regression equations. Nevertheless, in this study, only two equation models were selected (see table 3), because both presented the best performance in the research performed in the same study area by Poulain *et al*. (2010).

SR showed the strongest relationship with forest variables in a model using a single predictor. The RMSE value reported in this study (129.7 Mg ha^{-1} for AGTB and mean AGTB = 226.3 Mg ha^{-1}) is comparable to the value reported by Labrecque *et al*. (2006) for a hardwood/softwood boreal stand using the NIR band of Landsat TM data as a predictor in the same model (mean biomass = 125 Mg ha^{-1} and RMSE = 71 Mg ha^{-1}). Meanwhile, Eckert (2006) reported that biomass modelling based on spectral information performed only weakly for lenga stands. The highest R^2 (0.53) was found based on ASTER band 9, with the same model developed by Labrecque *et al*. (2006).

Model 2 (Muukkonen and Heiskanen 2005) showed the best results for the OBV, SB and AGTB estimation, always using SR and VCF as the predictors. The combination of per- and sub-pixel vegetation parameters (i.e. SR and VCF, respectively) is believed to enhance the estimation, as compared to the model with only one per-pixel parameter predictor.

The SR index measures the overall amount and quality of photosynthetic material in vegetation at the pixel level by rationing the near infrared wavelength band (wherein leaves of the canopy strongly reflect energy) and the red visible wavelength band (wherein chlorophyll pigments strongly absorb photons for storing energy through photosynthesis) (Aronoff 2005). Meanwhile, VCF measures the amount of the overall vegetation contained within a pixel. In contrast to per-pixel vegetation indices, the VCF yields an estimate of the approximate proportion of ground area occupied by vegetation in each pixel, describes the physical properties of the landscape and lends a straightforward interpretation based on established ecological knowledge (Purevdorj *et al*. 1998, Asner *et al*. 2003). Therefore, it is believed that the combination of per- and sub-pixel parameters (SR and VCF, respectively) renders a more complete characterization of the vegetation condition depicted in an image, which can enhance the values from the models. Moreover, since it has been pointed out that the selection of end members may be the most important aspect in the spectral mixture analysis (Lu *et al*. 2004), in this study only quite distinctive materials made up the few land-cover types (e.g. vegetation, bare soil, ice/snow, water), facilitating the interpretation of the end members and replication of this method in a large lenga forest with similar conditions.

Furthermore, the natural structure of the lenga forest consists of a mosaic of stands, often unevenly aged forest patches with homogenous within-stand structure (Schmidt and Urzúa 1982, Gea-Izquierdo *et al*. 2004). This condition can support good results in the equation models. Moreover, the study area includes primary and managed stands, and the stands managed under shelterwood cuts, as compared with the other stands, enhances this homogenous within-stand structure. Therefore, these managed

stands can present the best results in the equation models. Eckert (2006) indicated that since biomass estimation based on optical remote-sensing data is recognized as very difficult to achieve, promising results could be expected in areas with naturally occurring low woody biomass levels and slow accumulation rates. This argument could also be applied to patagonian *Nothofagus* forests.

4.4 *Biomass estimation*

Land use, land-use change and forestry are very uncertain emission categories (Monni *et al*. 2004). Incomplete information regarding the spatial distribution of carbon stored in biomass introduces substantial uncertainty to current estimation of the global carbon budget (Brown and Schroeder 1999). Monni *et al*. (2004) pointed out that uncertainty in carbon stock changes from some activities under Article 3.3 (afforestation and reforestation) and Article 3.4 (forest management) of the Kyoto Protocol range between 50% and 100%. Therefore, three approaches (tiers) for estimating carbon are proposed by the IPCC Good Practice Guidance (IPCC 2003). Tier 1 is based on default assumptions and default values of carbon stocks for example for different forest types. In tier 2, country-specific carbon stocks are applied to activity data, disaggregated to appropriate scales. In tier 3, countries use advanced estimation approaches that may involve complex models and highly disaggregated data including detailed maps based on remote sensing as well as *in-situ* measurements. Estimates of carbon provided by the Good Practice Guidance Tier 3 approach yield the lowest uncertainties, but involve local research and the highest costs.

The accuracy of estimating biomass based on forest inventory data and optical remote-sensing techniques can be improved by considering several aspects, such as: (1) measurement errors in the areas assigned to different land uses (for example, area estimates derived from traditional two-dimensional map projections often underestimate the true surface area (Zhao and Zhou 2006), influencing the accuracy of remotely sensed data); (2) forest inventory data, which includes only those trees with higher economic timber values and with diameters above a certain criteria (Feng *et al*. 1999, Zhao and Zhou 2005) (e.g. only those commercial trees with DBH $>$ 10 cm were surveyed in this study); (3) inherent errors from the diverse external data sources applied; and (4) co-registration of image data and field plots (Heiskanen 2006).

In sum, this research can be used to estimate biomass and carbon stock in a large forest area more precisely if the uncertainty of these remote-sensing estimates can be further reduced. Therefore, these results are important as the first step in the *Nothofagus pumilio* forest carbon assessment.

In this study, the accounting of the belowground biomass, coarse woody debris and underground biomass was not included, which must be included in the calculation of total forest biomass for analysing the change that is produced by the different silviculture management methods, especially in these forest components.

In forestry research studies, ASTER data have not been used as much as Landsat data. The widespread use of ASTER is hindered due to relatively small image size and non-systematic data collection (Heiskanen 2006). However, inherent advantages such as the fact that a primary goal of ASTER is to obtain a cloud-free map of the land surface during the mission (Yamaguchi *et al*. 1998) and improved spatial and spectral resolution should be taken into account. Furthermore, even if spectrally enhanced optical remote-sensing products, such as hyperspectral imagery, may significantly improve the precision of results related to this type of research, the data

acquisition, processing and analysis is easier for the ASTER multispectral scene, and it consequently facilitates their replication. Therefore, further research could improve the accuracy of the results in this study and include the components that were not accounted for, allowing for use in assessing temporal carbon change and land-use changes, whereas in this study, remotely sensed data have been used to map land cover and land-use change (Franklin *et al*. 2000, Puhr and Donoghue 2000).

5. Conclusions

The purpose of this study was to analyse the relationships between ASTER and intervened and non-intervened *Nothofagus pumilio* forest stand data in order to retrieve a biomass equation model that was extrapolated to an area located in the Magellan region, Chile. The results indicate that only VCF presented significant differences between the stand with shelterwood cuts (SC1 and SC2) and the other stands (P and E). Therefore, the research has shown that the spectral mixture analysis based on a linear unmixing model (which allows retrieval of VCF) can have better behaviours when applied to the estimation of biomass and volume. Further research should be attempted to analyse the applications of VCF in lenga forest because different techniques used to retrieve this vegetation parameter may introduce variations in the results. In these cases, spectral mixture analysis techniques offer a convenient alternative for tasks such as the accounting and monitoring of biomass and carbon stocks as well as analysing new intervention in primary lenga stands.

This study showed the potential of the combination of the SR and the VCF parameters to estimate the lenga forest biomass. However, as the actual coefficients of the equation model used are specific to this research, the equation models generated are limited to the site conditions and the species present in the given area. This result could be transferred to estimate biomass and volume in other *Nothofagus pumilio* forests with similar conditions. Moreover, it can be considered the first step in assessing temporal carbon storage change detections in a large area for this type of forests.

Even measuring biomass from satellite-derived multispectral data is unlikely to be as precise as forest inventories; the former is an adequate tool when complemented by the latter. It can be used to estimate changes and stocks in biomass in large and inaccessible areas. Furthermore, it is cheaper and faster than developing inventory data. To understand how forests contribute to the global carbon budget, it is necessary to understand the effect of forest management on carbon budgets over a range of temporal scales. The results obtained in this study provide information for biomass accounting and the management of lenga forests in the region, covering a research topic that now has significant interest in the context of climate change.

Acknowledgements

We would like to thank the companies, Forestal y Ganadera Monte Alto Ltda. and Salfa Corp. for allowing us to use their forests for this study. This study was carried out under a cooperative project between the Forest Science Faculty of the Universidad de Chile and the Wald-Zentrum of the Westfäliche Wilhelms-Universität Münster, supported by the Internationales Institut für Wald und Holz scholarship.

References

Aronoff, S., 2005, *Remote Sensing for GIS Managers*, p. 487 (New York: ESRI Press).

Asner, G., Hicke, J. and Lobell, D., 2003, Vegetation indices, spectral mixture analysis and canopy reflectance modeling. In *Remote Sensing of Forest Environments: Concepts and Case Studies*, M.A. Wulder and S.E. Franklin (Eds.), pp. 209–254 (Dordrecht: Kluwer Academic Publishers).

Birth, G.S. and McVey, G.R., 1968, Measuring the colour of growing turf with a reflectance spectrophotometer. *Agronomy Journal*, **60**, pp. 640–643.

Brown, D.G., 2001, A spectral unmixing approach to leaf area index (LAI) estimation at the alpine treeline ecotone. In *GIS and Remote Sensing Applications in Biogeography and Ecology*, A.C. Millington, S.J. Walsh and P.E. Osborne (Eds.), pp. 7–21 (Dordrecht: Kluwer Academic Publishers).

Brown, S., 2002, Measuring carbon in forests: current status and future challenges. *Environmental Pollution*, **116**, pp. 363–372.

Brown, S. and Schroeder, P., 1999, Spatial patterns of aboveground production and mortality of wood biomass for eastern U.S. Forests. *Ecological Applications*, **9**, pp. 968–980.

Caldentey, J., 1995, Acumulación de biomasa en rodales naturales de *Nothofagus pumilio* en Tierra del Fuego, Chile. *Investigación Agraria: Sistemas Y Recursos Forestales*, **4**, pp. 165–175 [in Spanish].

Caldentey, J., Mayer, H., Ibarra, M. and Promis, A., 2009, The effects of a regeneration felling on photosynthetic photon flux density and regeneration growth in a *Nothofagus pumilio* forest. *European Journal of Forest Research*, **128**, pp. 75–84.

Caldentey, J., Promis, A., Schmidt, H. and Ibarra, M., 2000, Variación Microclimática Causada por una Corta de Protección en un Bosque de lenga (*Nothofagus pumilio*). *Ciencias Forestales*, **14**, pp. 1999–2000 [in Spanish].

CONAF-CONAMA (Corporación Nacional Forestal – Corporación Nacional del Medio Ambiente), 1999, *Catastro y evaluación de recursos vegetacionales nativos de Chile. Proyecto CONAF-CONAMA-BIRF. Universidad Austral de Chile, Pontificia Universidad Católica de Chile y Universidad Católica de Temuco*, p. 89 (Santiago: CONAF-CONAMA) [in Spanish].

CONAF-CONAMA (Corporación Nacional Forestal - Corporación Nacional del Medio Ambiente), 2006, *Monitoreo y actualización. Catastro de uso del suelo y vegetación, Región de Magallanes y Antártica Chilena*, p. 14 (Santiago: CONAF-CONAMA) [in Spanish].

Davis, M.R., Allen, R.B. and Clinton, P.W., 2003, Carbon storage along a stand development sequence in a New Zealand *Nothofagus* forest. *Forest Ecology and Management*, **177**, pp. 313–321.

Eckert, S., 2006, A contribution to sustainable forest management in Patagonia – object-oriented classification and forest parameter extraction based on ASTER and Landsat ETM+ Data. PhD thesis, Department of Geography, University of Zurich, p. 154.

Feng, Z.W., Wang, X.K. and Wu, G., 1999, *Biomass and Net Primary Productivity of China's Forest Ecosystems*, pp. 49–50 (Beijing: Chinese Scientific Pressing House).

Franklin, J., Woodcock, C.E. and Warbington, R., 2000, Digital vegetation maps of forest lands in California: integrating satellite imagery, GIS modeling, and field data in support of resource management. *Photogrammetric Engineering and Remote Sensing*, **66**, pp. 1209–1217.

Gajardo, R., 1994, *La Vegetacion Natural De Chile. Clasificacion Y Distribucion Geografica*, p. 121 (Santiago: Editorial Universitaria) [in Spanish].

Gea-Izquierdo, G., Martínez Pastur, G., Cellini, J.M. and Lencinas, M.V., 2004, Forty years of silvicultural management in southern *Nothofagus pumilio* primary forests. *Forest Ecology and Management*, **201**, pp. 335–347.

Gitelson, A., Kaufman, Y.J. and Merzlyak, M.N., 1996, Use of a green channel in remote sensing of global vegetation from EOS-MODIS. *Remote Sensing of Environment*, **58**, pp. 289–298.

Gitelson, A., Kaufman, Y.J., Stark, R. and Rundquist, D., 2002, Novel algorithms for remote estimation of vegetation fraction. *Remote Sensing of Environment*, **80**, pp. 76–87.

Hart, P.B.S., Clinton, P.W., Allen, R.B., Nordmeyer, A.H. and Evans, G., 2003, Biomass and macro-nutrients (above- and below-ground) in a New Zealand beech (*Nothofagus*) forest ecosystem: implications for carbon storage and sustainable forest management. *Forest Ecology and Management*, **174**, pp. 281–294.

Heiskanen, J., 2006, Estimating aboveground tree biomass and leaf area index in a mountain birch forest using ASTER satellite data. *International Journal of Remote Sensing*, **27**, pp. 1135–1158.

IPCC (Intergovernmental Panel on Climate Change), 2003, Good practice guidance for land use, land-use change and forestry. IPCC National Greenhouse Gas Inventories Programme, p. 295 (Hayama: IPCC).

Klein, D., Fuentes, J.P., Schmidt, A., Schmidt, H. and Schulte, A., 2008a, Soil organic C as affected by silvicultural and exploitative interventions in *Nothofagus pumilio* forests of the Chilean Patagonia. *Forest Ecology and Management*, **255**, pp. 3549–3555.

Klein, D., Schmidt, A., Heim, M., Schmidt, H. and Schulte, A., 2008b, Das Totholzaufkommen in Lenga (*Nothofagus pumilio*)-Natur- und Wirtschaftswäldern sowie dessen Funktion als Kohlenstoffspeicher. *Forstarchiv*, **79**, pp. 8–54 [in German].

Krankina, O.N., Harmon, M.E., Cohen, W.B., Setter, D.R., Zyrina, O. and Duane, M., 2004, Carbon stores, sinks, and sources in forests of northwestern Russia: can we reconcile forest inventories with remote sensing results? *Climatic Change*, **67**, pp. 257–272.

Labrecque, S., Fournier, R.A., Luther, J.E. and Piercey, D., 2006, A comparison of four methods to map biomass from Landsat-TM and inventory data in western Newfoundland. *Forest Ecology and Management*, **226**, pp. 129–144.

Le Maire, G., François, C. and Dufrêne, E., 2004, Towards universal broad leaf chlorophyll indices using PROSPECT simulated database and hyperspectral reflectance measurements. *Remote Sensing of Environment*, **89**, pp. 1–28.

Lillesand, T.M., Kiefer, R.W. and Chipman, J.W., 2004, *Remote Sensing and Image Interpretation*, p. 763 (New York: John & Wiley Sons).

Loguercio, G., 2001, *Evaluación de los bosques de lenga de Tierra del Fuego como sumideros de carbono. Informe Final*, p. 58 (Argentina: Tierra del Fuego, Consejo Federal de Inversiones. Gobierno de Tierra del Fuego) [in Spanish].

Lu, D., Batistella, M., Moran, E. and Mausel, P., 2004, Application of spectral mixture analysis to Amazonian land-use and land-cover classification. *International Journal of Remote Sensing*, **25**, pp. 5345–5358.

Martínez-Pastur, G., Cellini, J.M., Peri, P.L., Vukasovic, R.F. and Fernández, M.C., 2000, Timber production of *Nothofagus pumilio* forests by a shelterwood system in Tierra del Fuego (Argentina). *Forest Ecology and Management*, **134**, pp. 153–162.

Monni, S., Syri, S., Pipatti, R. and Savolainen, I. 2004. Comparison of uncertainty in different emission trading schemes. In *Proceedings of the International Workshop on Uncertainty in Greenhouse Gas Inventories: Verification, Compliance and Trading*, 24–25 September 2004, Warsaw, Poland (Warsaw: Systems Research Institute), pp. 106–115.

Muukkonen, P. and Heiskanen, J., 2005, Estimating biomass for boreal forests using ASTER satellite data combined with standwise forest inventory data. *Remote Sensing of Environment*, **99**, pp. 434–447.

Muukkonen, P. and Heiskanen, J., 2007, Biomass estimation over a large area based on standwise forest inventory data and ASTER and MODIS satellite data: a possibility to verify carbon inventories. *Remote Sensing of Environment*, **107**, pp. 617–624.

Poulain, M., Peña, M., Schmidt, A., Schmidt, H. and Schulte, A., 2010, Relationships between forest variables and remote sensing data in a *Nothofagus pumilio* forest. *Geocarto International*, **25**, pp. 25–43.

Poulain, M., Prendez, M. and Sanhueza, E., 2008, Die regionale Treibhausgasbilanzierung für den Sector Landnutzungsänderung und Forswirschaft am Beispiel der XI. Region Aysén, Chile. *Forstarchiv*, **79**, pp. 40–47 [in German].

Puhr, C.B. and Donoghue, D.N.M., 2000, Remote sensing of upland conifer plantations using Landsat TM data: a case study from Galloway, south-west Scotland. *International Journal of Remote Sensing*, **21**, pp. 633–646.

Purevdorj, T.S., Tateishi, R., Ishiyama, T. and Honda, Y., 1998, Relationships between percent vegetation cover and vegetation indices. *International Journal of Remote Sensing*, **19**, pp. 3519–3535.

Rosenfeld, J.M., Navarro Cerrillo, R.M. and Guzman Alvarez, J.R., 2006, Regeneration of *Nothofagus pumilio* [Poepp. Et Endl.] Krasser forests after five years of seed tree cutting. *Journal of Environmental Management*, **78**, pp. 44–51.

Rouse, J.W.J., Haas, R.H., Schell, J.A. and Deering, D.W., 1973, Washington, DC, Monitoring vegetation systems in the Great Plains with ERTS. In *3th Earth Resources Technology Satellite-1 Symposium*, 10–14 December 1973, Washington, DC (Washington, DC: NASA), pp. 309–317.

Schmidt, A., Klein, D., Leuthold, F., Schmidt, H. and Schulte, A., 2008, Anteil der Wurzelbiomasse an der Gesamtbaumbiomasse eines Lenga (*Nothofagus pumilio*)-Naturwaldes im chilenischen Teil Patagoniens. *Forstarchiv*, **79**, pp. 55–59 [in German].

Schmidt, A., Poulain, M., Klein, D., Krause, K., Peña-Rojas, K., Schmidt, H. and Schulte, A., 2009, Allometric above-belowground biomass equations for *Nothofagus pumilio* natural regeneration in the Chilean Patagonia. *Annals of Forest Science*, **66**, pp. 513–520.

Schmidt, H., Cruz, G., Promis, A. and Alvarez, M., 2003, Transformacion de los bosques de lenga virgenes e intervenidos a bosques manejados. *Universidad de Chile, Facultad de Ciencias Forestales. Publicaciones Miscelaneas Forestales*, **14**, p. 60 [in Spanish].

Schmidt, H. and Urzúa, A., 1982, Transformación y manejo de los bosques de lenga en Magallanes. *Ciencias Agrarias*, **11**, pp. 1–62 [in Spanish].

Schulte, A., 2001, Weltforstwirtschaft und Klimawandel: Globale Trends und Interdependenzen. In *Weltforstwirtschaft nach Kyoto: Wald und Holz Als Kohlenstoffspeicher und Regenerativer Energieträger*, A. Schulte, K. Böswald and R. Joosten (Eds.), pp. 1–21 (Aachen: Shaker) [in German].

Treitz, P.M. and Howarth, P.J., 1999, Hyperspectral remote sensing for estimating biophysical parameters of forest ecosystems. *Progress in Physical Geography*, **23**, pp. 359–390.

Veblen, T.T., Hill, R.S. and Read, J., 1996, *The Ecology and Biogeography of Nothofagus Forests*, p. 403 (New Haven: Yale University Press).

Weber, M., 2001, *Kohlenstoffspeicherung in Lenga- (Nothofagus pumilio) Primärwäldern Feuerlands und Auswirkungen ihrer Überführung in Wirtschafswald auf den C-Haushalt*, p. 119 (Germany: Verlag Dr. Norber Kessel) [in German].

Wulder, M.A., Skakun, R.S., Kurz, W.A. and White, J.C., 2004, Estimating time since forest harvest using segmented Landsat ETM+ imagery. *Remote Sensing of Environment*, **93**, pp. 79–187.

Yamaguchi., Y., Kahle., A., Tsu., H., Kawakami., T. and Pniel, M., 1998, Overview of Advance Spaceborne Thermal Emission and Reflection Radiometer (ASTER). *IEEE Transactions on Geoscience and Remote Sensing*, **36**, pp. 1062–1071.

Zhao, M. and Zhou, G.S., 2005, Estimation of biomass and net primary productivity of major planted forests in China based on forest inventory data. *Forest Ecology and Management*, **207**, pp. 295–313.

Zhao, M. and Zhou, G.S., 2006, Estimating net primary productivity of Chinese pine forests based on forest inventory data. *Forestry*, **79**, pp. 231–239.

Zianis, D. and Mencuccini, M., 2003, Aboveground biomass relationships for beech (*Fagus moesiaca* Cz.) trees in Vernio Mountain, Northern Greece, and generalised equations for *Fagus* sp. *Annals of Forest Science*, **60**, pp. 439–448.